Article

# A close quasar pair in a disk–disk galaxy merger at $z = 2.17$

https://doi.org/10.1038/s41586-023-05766-6

Received: 13 September 2022

Accepted: 26 January 2023

Published online: 5 April 2023

Check for updates

**Yu-Ching Chen[1,2], Xin Liu[1,2] ✉, Adi Foord[3], Yue Shen[1,2], Masamune Oguri[4,5], Nianyi Chen[6], Tiziana Di Matteo[6,7,8], Miguel Holgado[6], Hsiang-Chih Hwang[9] & Nadia Zakamska[10]**

Galaxy mergers produce pairs of supermassive black holes (SMBHs), which may be witnessed as dual quasars if both SMBHs are rapidly accreting. The kiloparsec (kpc)-scale separation represents a physical regime sufficiently close for merger-induced effects to be important[1] yet wide enough to be directly resolvable with the facilities currently available. Whereas many kpc-scale, dual active galactic nuclei—the low-luminosity counterparts of quasars—have been observed in low-redshift mergers[2], no unambiguous dual quasar is known at cosmic noon ($z \approx 2$), the peak of global star formation and quasar activity[3,4]. Here we report multiwavelength observations of Sloan Digital Sky Survey (SDSS) J0749 + 2255 as a kpc-scale, dual-quasar system hosted by a galaxy merger at cosmic noon ($z = 2.17$). We discover extended host galaxies associated with the much brighter compact quasar nuclei (separated by 0.46″ or 3.8 kpc) and low-surface-brightness tidal features as evidence for galactic interactions. Unlike its low-redshift and low-luminosity counterparts, SDSS J0749 + 2255 is hosted by massive compact disk-dominated galaxies. The apparent lack of stellar bulges and the fact that SDSS J0749 + 2255 already follows the local SMBH mass–host stellar mass relation, suggest that at least some SMBHs may have formed before their host stellar bulges. While still at kpc-scale separations where the host-galaxy gravitational potential dominates, the two SMBHs may evolve into a gravitationally bound binary system in around 0.22 Gyr.

Sloan Digital Sky Survey (SDSS) J0749 + 2255 is an optically selected type 1 (that is, broad-line) quasar at $z = 2.17$ spectroscopically confirmed by the SDSS legacy survey[5]. It was selected as a candidate kpc-scale, dual quasar using Gaia astrometry[6]. Hubble Space Telescope (HST) optical dual-band imaging of SDSS J0749 + 2255 has shown compact double nuclei with a projected nuclear angular separation of 0.46″ (ref. [7]). Close compact optical double nuclei could represent a dual quasar, a projected quasar pair in two noninteracting galaxies, a strongly lensed quasar or a star-quasar superposition. Previous very-long-baseline array 15.0 GHz (Ku-band) imaging detected strong radio emissions from both nuclei, ruling out star-quasar superposition[7]. Whereas morphological differences in the very-long-baseline array 15.0 GHz image of the two radio nuclei favour a dual quasar or a premerger projected quasar pair at larger physical separations, strong lensing could not be conclusively ruled out[7].

To unambiguously test the nature of SDSS J0749 + 2255, we have conducted a comprehensive multiwavelength follow-up campaign. The new observations include HST infrared (IR) F160W (H-band) imaging, Keck adaptive optics (AO)-assisted IR ($K_p$-band) imaging, HST/Space Telescope Imaging Spectrograph (STIS) optical spatially resolved slit spectroscopy, Gemini spatially resolved optical (GMOS) and near infrared (NIR) (GNIRS) slit spectroscopy, Chandra Advanced CCD Imaging Spectrometer (ACIS)-S X-ray 0.5–8.0 keV imaging spectroscopy and very-large array (VLA) A-configuration (A-config) radio dual-band (15 and 6 GHz) imaging. These multiwavelength observations establish SDSS J0749 + 2255 as a dual quasar hosted by an ongoing galaxy merger at $z = 2.17$.

First, after we subtract the bright central quasars modelled by two point-spread functions (PSFs), the deep HST IR image uncovers two extended host galaxies underlying both compact quasar nuclei (Fig. 1). In addition, after we further subtract the best axisymmetric models for the extended host galaxies, the final residual image shows low-surface-brightness tidal features indicative of mergers (Fig. 1). Detection of these faint tidal features is of great significance (over $10\sigma$ for each integrated feature; Supplementary Information). Detecting both tidal features and the extended host galaxies unambiguously confirms SDSS J0749 + 2255 as a dual quasar in a merger rather than a strongly lensed quasar or a premerger projected quasar pair at larger physical separations. Complementary higher-angular-resolution Keck AO-assisted IR imaging independently supports the detection of the extended host galaxies and the nondetection of a central foreground lens galaxy. The alternative scenario of a foreground lens galaxy

[1]Department of Astronomy, University of Illinois at Urbana-Champaign, Urbana, IL, USA. [2]National Center for Supercomputing Applications, University of Illinois at Urbana-Champaign, Champaign, IL, USA. [3]Kavli Institute of Particle Astrophysics and Cosmology, Stanford University, Stanford, CA, USA. [4]Center for Frontier Science, Chiba University, Chiba, Japan. [5]Department of Physics, Graduate School of Science, Chiba University, Chiba, Japan. [6]McWilliams Center for Cosmology, Department of Physics, Carnegie Mellon University, Pittsburgh, PA, USA. [7]NSF AI Planning Institute for Physics of the Future, Carnegie Mellon University, Pittsburgh, PA, USA. [8]OzGrav-Melbourne, Australian Research Council Centre of Excellence for Gravitational Wave Discovery, Melbourne, Victoria, Australia. [9]School of Natural Sciences, Institute for Advanced Study, Princeton, NJ, USA. [10]Department of Physics and Astronomy, Johns Hopkins University, Baltimore, MD, USA. ✉e-mail: xinliuxl@illinois.edu

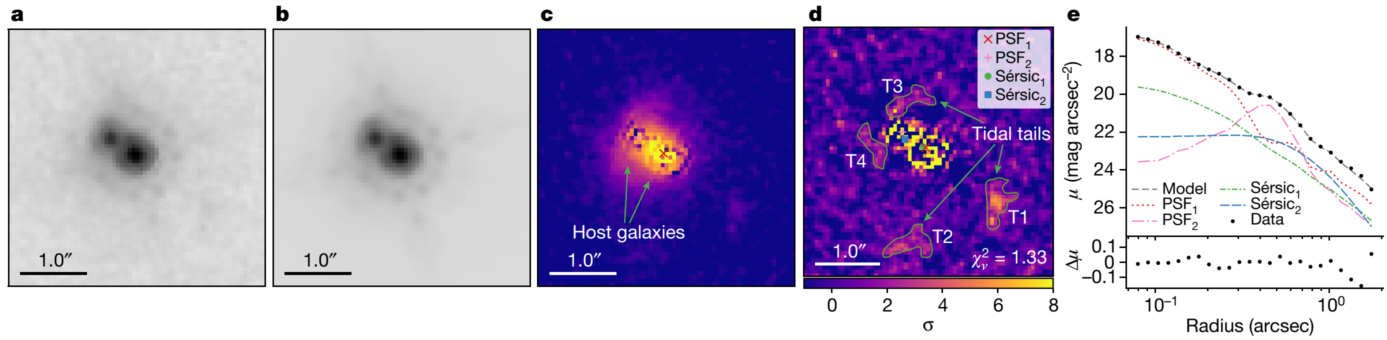


**Fig. 1 | HST imaging. a–e**, HST/WFC3 F160W (H-band) image and two-dimensional structural decomposition results using GALFIT[31] modelling for SDSS J0749 + 2255. **a**, Raw HST image. **b**, Our best-fit model consisting of two PSFs for the central quasars and two Sérsic models for the two host galaxies. **c**, Two-PSF-subtracted image highlighting the detection of two host galaxies underlying both quasars in the merger. **d**, Residual image after subtraction of two PSFs and two Sérsic models, showing detection of low-surface-brightness tidal tails indicative of ongoing galactic interactions. **e**, One-dimensional radial profiles of the data and best-fit model and their individual components. Detection of both host galaxies and tidal tails unambiguously confirms the system as a dual quasar rather than a lensed quasar or a premerger projected quasar pair at larger physical separations. In addition to the two Sérsic models for the two quasar host galaxies, we have also considered the alternative scenario of a single Sérsic model for a central foreground lens galaxy, which is disfavoured by the data based on the reduced chi-squared $(\chi^2_\nu)$ values. $\mu$, surface brightness.

as a single extended source located between two compact quasar nuclei is quantitatively ruled out by strong lensing mass model tests (Supplementary Information). However, the tidal features seen in the HST image are too faint to detect in the shallower Keck AO image.

Second, Chandra ACIS-S detects both quasar nuclei in hard X-rays (2–8 keV) as compact X-ray point sources whose spatial profiles are consistent with the PSF (Fig. 2). The X-ray positional offsets between the two nuclei are consistent with those of the HST optical nuclei. The optically fainter northeast (NE) nucleus is brighter in the X-rays than the southwest (SW) nucleus. This contradicts naive expectations from a strongly lensed quasar, because gravitational lensing is in general achromatic: the deflection angle of a light ray (and the lensing magnification) does not depend on its wavelength, so consistent flux ratios are expected at different wavelengths from different-lensed images given the same underlying source spectrum. Whereas the wavelength-dependent geometry of the different emission regions may result in chromatic effects[8], differences in flux ratios between different images at different wavelengths should be minor in a strongly lensed quasar. However, the 2–8 keV X-ray flux ratio between the two nuclei (NE/SW) is $45^{+41}_{-33}$, which is significantly different from that observed by HST in the optical (0.229 ± 0.001 in F475W and 0.284 ± 0.002 in F814W), disfavouring strong lensing. A caveat is that microlensing can cause such flux ratio anomalies given the different optical and X-ray-emitting region sizes frequently observed[9–11], although the discrepancy for SDSS J0749 + 2255 is seen as extreme. The X-ray-to-optical luminosity ratio typically characterized by the spectral slopes $\alpha_{\rm OX}$ is 1.46 ± 0.01 for the NE nucleus and 2.32 ± 0.13 for the SW nucleus (Supplementary Information). The estimated unabsorbed hard X-ray (2–8 keV) luminosities (assuming a redshift of $z$ = 2.17 for both X-ray point sources) are approximately $10^{45.29^{+0.05}_{-0.03}}$ erg s$^{-1}$ for the NE nucleus and approximately $10^{43.62^{+0.32}_{-0.58}}$ erg s$^{-1}$ for the SW nucleus, both greatly exceeding the most X-ray-luminous starburst galaxies[12]. We also find significantly different intrinsic absorbing columns in the two nuclei ($4.7^{+1.3}_{-2.6} \times 10^{22}$ cm$^{-2}$ for the NE nucleus and below $10^{20}$ cm$^{-2}$ for the SW nucleus), lending further support to the dual-quasar hypothesis.

Third, both quasar nuclei are detected as compact radio sources by VLA A-config continuum imaging at 6 and 15 GHz (Fig. 3). The radio point source centres are consistent with those of the HST optical quasar nuclei. Radio flux ratios between the two nuclei (NE/SW) are 0.379 ± 0.001 at 6 GHz and 0.351 ± 0.003 at 15 GHz, which are different (by over 5$\sigma$) than those observed by HST in the optical (0.229 ± 0.001 in F475W and 0.284 ± 0.002 in F814W), disfavouring strong lensing but with the caveat of flux ratio anomalies caused by microlensing. The radio spectral indices are −0.397 ± 0.004 for the NE nucleus and −0.314 ± 0.002 for the SW nucleus. The radio loudness parameter, $R_{6\,{\rm cm}/2{,}500\,{\rm \AA}}$, commonly defined as the flux density ratio at the rest-frame 6 cm and that at 2,500 Å, is 1,079 ± 74 for the NE nucleus and 659 ± 16 for the SW nucleus, placing both quasars in the radio-loud (that is, $R_{6\,{\rm cm}/2{,}500\,{\rm \AA}}$ over 10) population according to the canonical definition[13].

Finally, HST spatially resolved optical spectroscopy shows significantly different rest-frame ultraviolet continuum spectral slopes between the two nuclei ($\alpha_\nu$ = −0.70 ± 0.24 for the NE nucleus and 0.08 ± 0.06 for the SW nucleus), independently confirmed by Gemini/GMOS spatially resolved optical slit spectroscopy (Fig. 4). However, the GMOS spectra are only marginally resolved for the two nuclei and hence the spectral slope measurements are not as reliable as the HST-based results. The different spectral slopes disfavour a strongly lensed quasar, although strong gravitational lenses may also produce different spectral slopes due to varying reddening along different light paths through the foreground lens galaxy[14]. There are noticeable differences in the broad emission lines, but the low spectroscopic data quality cannot conclusively rule out strong lensing based on the line shapes alone. The best-fit systemic redshifts estimated from the optical-IR spectra of the two quasar nuclei suggest a line-of-sight velocity offset of roughly 310 ± 50 km s$^{-1}$ (Supplementary Table 1), consistent with expectations of typical orbital velocities in galaxy mergers[15] but inconsistent with strong lensing (which would produce identical redshifts of the two quasars).

By modelling the PSF-subtracted, host-galaxy-only, two-band (HST F160W and Keck AO $K_p$) photometry of SDSS J0749 + 2255, we estimate the stellar masses of the two host galaxies at around $10^{11.46^{+0.02}_{-0.26}} M_\odot$ and $10^{11.50^{+0.04}_{-0.27}} M_\odot$ (with the errors accounting for the 1$\sigma$ statistical and partial systematic uncertainties from surface brightness profile fitting but ignoring additional systematics from population synthesis modelling) for the NE and SW nuclei. The massive hosts appear to be compact and disk dominated (with best-fit Sérsic indices close to unity; Supplementary Information), typical of galaxies[16] and hosts of single quasars[17] at $z > 2$. The disk dominance of the hosts in SDSS J0749 + 2255 is dramatically different from the more bulge-dominated characteristics of low-redshift, low-luminosity dual active galactic nucleus hosts[18]. The latter may be more subject to the stabilization effect of stellar bulges preventing more efficient SMBH fuelling in the early merging stages, resulting in low-luminosity active galactic nuclei rather than the luminous quasars observed in SDSS J0749 + 2255.

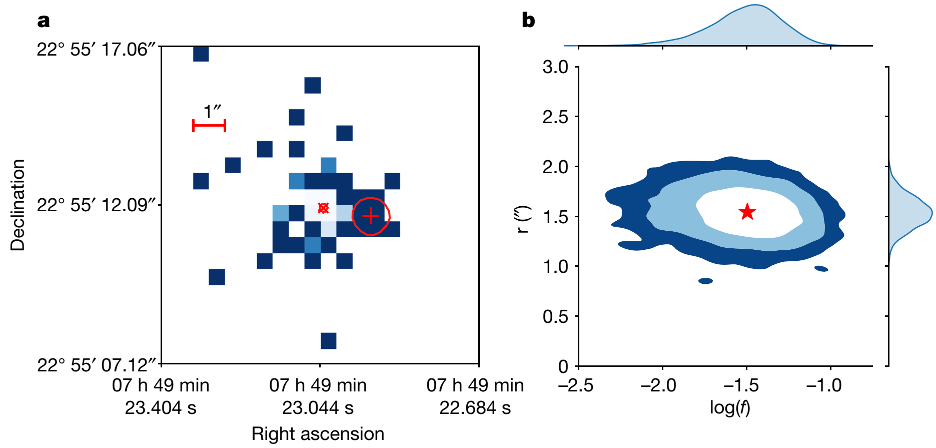


**Fig. 2 | X-ray imaging. a,b**, Chandra ACIS-S X-ray image and best-fit Bayesian AnalYsis of Multiple AGN in X-rays (BAYMAX) results for SDSS J0749 + 2255. **a**, Binned Chandra data (0.5–8.0 keV), centred on the nominal X-ray coordinates of quasar with best-fit locations of primary X-ray point source (red 'x') and secondary X-ray point source (red '+'), with 95% confidence interval in red contour. **b**, Joint-posterior distribution of the separation ($r$, in arcseconds) and count ratio (log($f$), ratio between the number of counts associated with secondary versus primary). Blue contour levels represent 68% and 95% confidence interval. We find the best-fit separation $r = 1.54''^{+0.39''}_{-0.36''}$ and $\log(f) = -1.43^{+0.30}_{-0.30}$ at the 95% confidence interval. Although the estimated separation is statistically larger than that estimated from HST imaging (0.46″), the estimated position angle between the two X-ray point sources ($350^{+37}_{-24}$°, 95% confidence interval) is consistent with that of the two resolved cores resolved in the HST imaging (330°).

By joint modelling of the optical-NIR spectrum (Supplementary Information), we estimate the SMBH masses as around $10^{9.1\pm0.4}M_\odot$ and roughly $10^{9.2\pm0.4}M_\odot$ (with errors representing 1$\sigma$ total uncertainties) for the NE and the SW nuclei, respectively. Bolometric luminosities estimated from the optical continua suggest Eddington ratios of about 0.12 ± 0.03 and 0.25 ± 0.07 for the NE and SW nuclei, respectively. SMBH masses and host total stellar masses are consistent with the empirical scaling relations observed in both single quasars at $z \approx 2$ and local inactive galaxies within uncertainties (Supplementary Information).

SDSS J0749 + 2255 represents a robust example of a kpc-scale pair of SMBHs in a galaxy merger at cosmic noon. It fills a long-standing gap in the expected population of dual quasars hosted by high-redshift ongoing galaxy mergers. Such systems are expected to be common in hierarchical merger models, which have otherwise been successful in explaining much of the quasar phenomenology[1]. In comparison, the previous redshift record holder of kpc-scale dual quasars hosted by confirmed galaxy mergers was LBQS 0103 − 2753 at $z = 0.86$, which was serendipitously discovered[19].

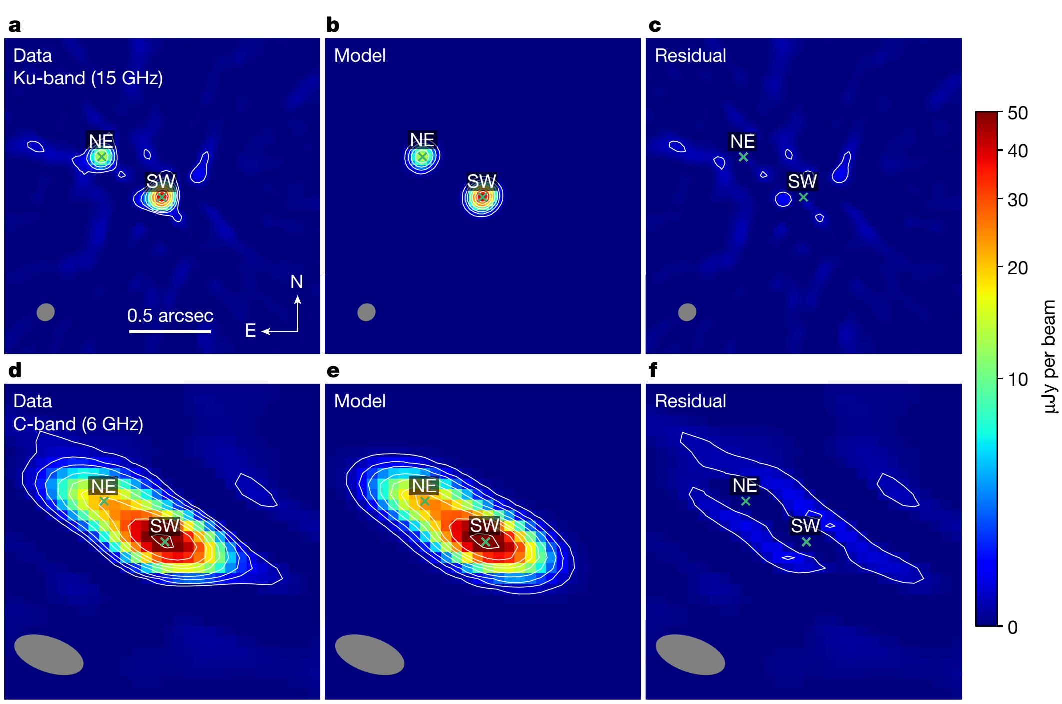


**Fig. 3 | Radio imaging. a–f**, VLA A-config Ku-band (**a**) and C-band (**d**) continuum images for SDSS J0749 + 2255. **b**,**c**, The Ku-band model (**b**) and residual (**c**) images. **e**,**f**, The C-band model (**e**) and residual (**f**) images. Contours represent 10, 30, 60, 120, 200, 300, 400, 600 and 1,000 × 1$\sigma$ noise levels. Green crosses denote centroids of the fitted Gaussian components. The synthesized beam sizes are shown in grey in the bottom left-hand corner. The restoring beam sizes are 0.11″ × 0.10″ (position angle (PA) = −54.0°) in the Ku-band and 0.44″ × 0.21″ (PA = 70.9°) in the C-band. The root mean square noise levels are 8.2 μJy per beam in the Ku-band and 5.3 μJy per beam in the C-band.

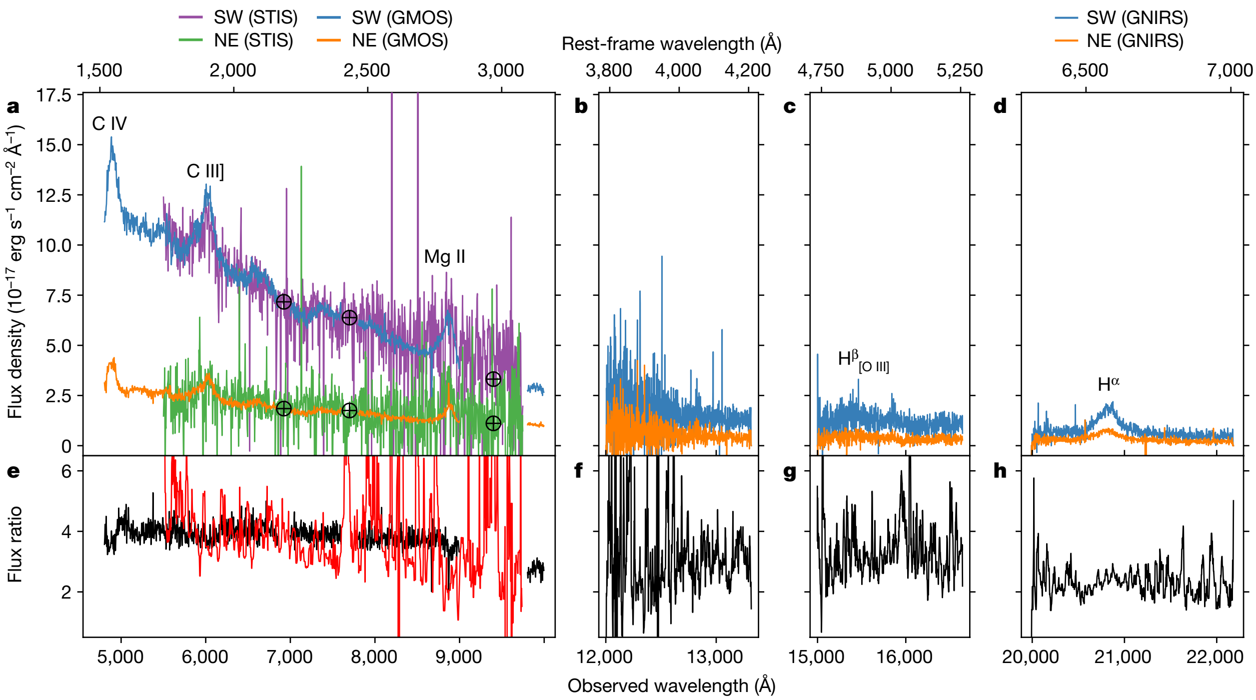


**Fig. 4 | Optical and NIR spectroscopy. a**–**d**, Spatially resolved optical (**a**) and NIR (**b** for J-band, **c** for H-band, and **d** for K-band) spectroscopy from HST/STIS (**a**), Gemini/GMOS (**a**) and Gemini/GNIRS (**b**–**d**) for SDSS J0749 + 2255. Orange and cyan curves represent Gemini spectra for the NE and SW nuclei, respectively; green and magenta curves represent HST spectra for the NE and SW nuclei, respectively. Labelled are the major strong emission lines detected. Circled cross symbols denote the telluric absorption region. **e**–**h**, Flux ratios between the two nuclei, with the HST-based flux ratio shown in red (**e**) and the Gemini-based flux ratio (for both GMOS (**e**) and GNIRS (**f**–**h**)) in black. The two nuclei have significantly different rest-frame UV continuum spectral slopes and strengths of the broad and narrow emission lines. The discrepancy between STIS- and GMOS-based flux ratios is probably caused by differences in slit coverage and/or observation time. We adopt STIS spectra to estimate the continuum power-law spectral indices, because STIS cleanly separated the two nuclei.

A handful of galactic-scale (below 10 kpc) dual quasar candidates were known at $z > 1$ (refs. [7,20–27]). However, none of these has been confirmed to be hosted by ongoing galaxy mergers—as expected in bona fide dual quasars (Supplementary Information). The establishment of SDSS J0749 + 2255 as a dual quasar hosted in a galaxy merger conclusively demonstrates that at least some high-redshift, kpc-scale, dual-quasar candidates may indeed be dual quasars rather than gravitational lenses or premerger projected quasar pairs at large separations. On larger (that is, over 10 kpc) scales, it has long been suggested that most wide-separation (3″ – 10″) double quasars are quasar pairs rather than gravitational lenses based on statistical arguments[28]. There are approximately tens of known 'binary' quasars at $z > 1$ with projected separations of over 10 kpc[29], and even a quasar 'quartet'[30]. However, the separations of most of these systems are still too large (approximately over tens of kpc) for the host galaxies of the quasar pair to be in direct galactic interactions. Unlike SDSS J0749 + 2255, none of these has been observed with tidal features as direct evidence for ongoing interactions.

Despite significant merit and intense theoretical interest, direct evidence for compact binary SMBHs—SMBHs that are gravitationally bound to each other—is still lacking[2]. Their separations (typically less than a few parsecs) are too small to resolve beyond the local universe with current facilities. High-redshift, kpc-scale, dual quasars represent promising progenitors of low-redshift compact binary SMBHs. Using a stellar dynamical friction argument, we estimate that the 3.8 kpc SMBH pair in SDSS J0749 + 2255 may form a compact bound SMBH binary in fewer than approximately $0.22^{+0.50}_{-0.16}$ Gyr (Supplementary Information). Future infrared integral field unit spectroscopy with the James Webb Space Telescope will map the stellar and gas kinematics, enabling better predictions on the subsequent SMBH pair orbital evolution and the impact of dual quasar on their host galaxies.

The confirmation of SDSS J0749 + 2255 as a dual quasar provides a proof of concept for combining multiwavelength facilities to discover high-redshift, kpc-scale dual quasars[7]. The discovery underscores the need for high-resolution deep NIR imaging, which is crucial for detection of merging galaxy hosts and for robust distinguishing of high-redshift dual quasars from lensed quasars and premerger projected quasar pairs at larger physical separations. Future high-resolution, wide-area deep surveys will uncover a larger sample of high-redshift dual quasars at the peak epoch of galaxy and SMBH assembly.

## Online content

Any methods, additional references, Nature Portfolio reporting summaries, source data, extended data, supplementary information, acknowledgements, peer review information; details of author contributions and competing interests; and statements of data and code availability are available at https://doi.org/10.1038/s41586-023-05766-6.


1. Hopkins, P. F., Hernquist, L., Cox, T. J. & Kereš, D. A cosmological framework for the co-evolution of quasars, supermassive black holes, and elliptical galaxies. I. Galaxy mergers and quasar activity. *Astrophys. J. Suppl. Ser.* **175**, 356–389 (2008).
2. Bogdanović, T., Miller, M. C. & Blecha, L. Electromagnetic counterparts to massive black-hole mergers. *Living Rev. Relativ.* **25**, 3 (2022).
3. Richards, G. T. et al. The Sloan Digital Sky Survey Quasar Survey: quasar luminosity function from data release 3. *Astron. J.* **131**, 2766–2787 (2006).
4. Madau, P. & Dickinson, M. Cosmic star-formation history. *Annu. Rev. Astro. Astrophys.* **52**, 415–486 (2014).
5. Schneider, D. P. et al. The Sloan Digital Sky Survey Quasar Catalog. V. Seventh data release. *Astron. J.* **139**, 2360–2373 (2010).
6. Hwang, H.-C., Shen, Y., Zakamska, N. & Liu, X. Varstrometry for off-nucleus and dual subkiloparsec agn (VODKA): methodology and initial results with gaia dr2. *Astrophys. J.* **888**, 73 (2020).
7. Shen, Y. et al. A hidden population of high-redshift double quasars unveiled by astrometry. *Nat. Astron.* **5**, 569–574 (2021).

8. Barnacka, A., Geller, M. J., Dell'Antonio, I. P. & Benbow, W. Strong gravitational lensing as a tool to investigate the structure of jets at high energies. *Astrophys. J.* **788**, 139 (2014).
9. Chang, K. & Refsdal, S. Flux variations of qso 0957 561 a, b and image splitting by stars near the light path. *Nature* **282**, 561–564 (1979).
10. Wambsganss, J. & Paczynski, B. Expected color variations of the gravitationally microlensed qso 2237+0305. *Astron. J.* **102**, 864–868 (1991).
11. Pooley, D., Blackburne, J. A., Rappaport, S., Schechter, P. L. & Fong, W.-f A strong X-ray flux ratio anomaly in the quadruply lensed quasar PG 1115+080. *Astrophys. J.* **648**, 67–72 (2006).
12. Zezas, A., Alonso-Herrero, A. & Ward, M. J. Searching for X-ray luminous starburst galaxies. *Astrophys. Space Sci.* **276**, 601–607 (2001).
13. Kellermann, K. I., Sramek, R., Schmidt, M., Shaffer, D. B. & Green, R. VLA observations of objects in the Palomar Bright Quasar Survey. *Astron. J.* **98**, 1195–1207 (1989).
14. Sluse, D., Hutsemékers, D., Courbin, F., Meylan, G. & Wambsganss, J. Microlensing of the broad line region in 17 lensed quasars. *Astron. Astrophys.* **544**, A62 (2012).
15. Contreras-Santos, A. et al. Galaxy pairs in The Three Hundred simulations: a study on the performance of observational pair-finding techniques. *Mon. Not. R. Astron. Soc.* **515**, 5375–5388 (2022).
16. Shapley, A. E. Physical properties of galaxies from $z=2$ to 4. *Annu. Rev. Astron. Astrophys.* **49**, 525–580 (2011).
17. Ding, X., Silverman, J. D. & Onoue, M. Opening the era of quasar-host studies at high redshift with JWST. *Astrophys. J. Lett.* **939**, L28 (2022).
18. Shangguan, J. et al. Chandra X-ray and Hubble Space Telescope imaging of optically selected kiloparsec-scale binary active galactic nuclei. II. Host galaxy morphology and AGN activity. *Astrophys. J.* **823**, 50 (2016).
19. Shields, G. A. et al. LBQS 0103-2753: a binary quasar in a major merger. *Astrophys. J.* **744**, 151 (2012).
20. Inada, N. et al. The sloan digital sky survey quasar lens search. ii. Statistical lens sample from the third data release. *Astron. J.* **135**, 496–511 (2008).
21. Schechter, P. L. et al. First lensed quasar systems from the vst-atlas survey: one quad, two doubles, and two pairs of lensless twins. *Astron. J.* **153**, 219 (2017).
22. Anguita, T. et al. The strong lensing insights into the dark energy survey (strides) 2016 follow-up campaign – ii. New quasar lenses from double component fitting. *Mon. Not. R. Astron. Soc.* **480**, 5017–5028 (2018).
23. Lemon, C. A., Auger, M. W., McMahon, R. G. & Ostrovski, F. Gravitationally lensed quasars in Gaia – II. Discovery of 24 lensed quasars. *Mon. Not. R. Astron. Soc.* **479**, 5060–5074 (2018).
24. Lemon, C. et al. The strong lensing insights into the dark energy survey (strides) 2017/2018 follow-up campaign: discovery of 10 lensed quasars and 10 quasar pairs. *Mon. Not. R. Astron. Soc.* **494**, 3491–3511 (2020).
25. Tang, S. et al. Optical spectroscopy of dual quasar candidates from the Subaru HSC-SSP program. *Astrophys. J.* **922**, 83 (2021).
26. Yue, M., Fan, X., Yang, J. & Wang, F. A candidate kiloparsec-scale quasar pair at $z=5.66$. *Astrophys. J. Lett.* **921**, L27 (2021).
27. Lemon, C. et al. J1721+8842: a gravitationally lensed binary quasar with a proximate damped lyman-$\alpha$ absorber. *Astron. Astrophys.* **657**, A113 (2022).
28. Kochanek, C. S., Falco, E. E. & Muñoz, J. A. Why quasar pairs are binary quasars and not gravitational lenses. *Astrophys. J.* **510**, 590–596 (1999).
29. Hennawi, J. F. et al. Binary quasars at high redshift. I. 24 New quasar pairs at $z \sim 3$-4. *Astrophys. J.* **719**, 1672–1692 (2010).
30. Hennawi, J. F., Prochaska, J. X., Cantalupo, S. & Arrigoni-Battaia, F. Quasar quartet embedded in giant nebula reveals rare massive structure in distant universe. *Science* **348**, 779–783 (2015).
31. Peng, C. Y., Ho, L. C., Impey, C. D. & Rix, H.-W. Detailed decomposition of galaxy images. II. Beyond axisymmetric models. *Astron. J.* **139**, 2097–2129 (2010).

**Publisher's note** Springer Nature remains neutral with regard to jurisdictional claims in published maps and institutional affiliations.

## Data availability

The SDSS spectrum (Plate, 1,203; FibreID, 576; MJD, 52669) is publicly available at https://www.sdss.org/. The HST, Chandra, VLA, Gemini and Keck data are all available through their separate public data archives (HST programme nos. GO-16210 and GO-16892, Chandra GO-23700377, VLA 20B-242, Gemini 2020B-FT-113 and 2022A-Q-139). Source data are provided with this paper.

## Code availability

The code used to model the HST and Keck data is publicly available at https://users.obs.carnegiescience.edu/peng/work/galfit/galfit.html. The code used for the lensing mass modelling test is publicly available at https://github.com/oguri/glafic2. The code used to perform the optical-NIR spectroscopic analysis is publicly available at https://github.com/legolason/PyQSOFit. The BAYMAX code used to model the Chandra data is available on reasonable request.

**Acknowledgements** We thank A. Kemball and A. Gross for helpful discussions on strong lensing. We thank M. Leveille, A. Vick, R. Campbell, R. McGurk, J. Cortes, T. R. Geballe, S. Leggett, A. Nitta, T. Seccull and H. Medlin for their help with our HST, Keck, Gemini and VLA observations. Y.-C.C. thanks J. Li and H. Guo for their help with the GALFIT and PyQSOFit codes. M.O. acknowledges support from JSPS KAKENHI grant nos. JP20H00181, JP20H05856 and JP22H01260. This work is supported by the Heising-Simons Foundation and Research Corporation for Science Advancement and National Science Foundation (NSF) grant nos. AST-2108162 and AST-2206499. This research was supported in part by the NSF under no. PHY-1748958. Support for programme no. 23700237 was provided by NASA through Chandra Award no. GO2-23099X issued by the Chandra X-ray Observatory Center, which is operated by the Smithsonian Astrophysical Observatory for and on behalf of NASA under contract no. NAS 8-03060. Support for programme nos. HST-GO-15900 (principal investigator (PI): H. Hwang), HST-GO-16210 and HST-GO-16892 was provided by NASA through grants from the Space Telescope Science Institute, which is operated by the Association of Universities for Research in Astronomy, Incorporated, under NASA contract no. NAS5-26555. The National Radio Astronomy Observatory is a facility of the NSF operated under cooperative agreement by Associated Universities, Inc. Based in part on data obtained at the W. M. Keck Observatory, which is operated as a scientific partnership among the California Institute of Technology, the University of California and the National Aeronautics and Space Administration. The Observatory was made possible by the generous financial support of the W. M. Keck Foundation. This research has made use of the Keck Observatory Archive, which is operated by the W. M. Keck Observatory and the NASA Exoplanet Science Institute, under contract with the National Aeronautics and Space Administration. We wish to recognize and acknowledge the very significant cultural role and reverence that the summit of Maunakea has always had within the indigenous Hawaiian community. We are most fortunate to have the opportunity to conduct observations from this mountain. Based in part on observations obtained at the international Gemini Observatory (programme nos. 2020B-FT-113 and GN-2022A-Q-139; PI: X. Liu), a programme of NSF's NOIRLab, which is managed by the Association of Universities for Research in Astronomy under a cooperative agreement with the NSF on behalf of the Gemini Observatory partnership: the NSF (USA), National Research Council (Canada), Agencia Nacional de Investigación y Desarrollo (Chile), Ministerio de Ciencia, Tecnología e Innovación (Argentina), Ministério da Ciência, Tecnologia, Inovações e Comunicações (Brazil) and Korea Astronomy and Space Science Institute (Republic of Korea). This work was enabled by observations made from the Gemini North telescope, located within the Maunakea Science Reserve and adjacent to the summit of Maunakea. We are grateful for the privilege of observing the Universe from a place that is unique in both its astronomical quality and cultural significance. This work makes use of SDSS-I/II and SDSS-III/IV data (http://www.sdss.org/ and http://www.sdss3.org/, respectively).

**Author Contributions** Y.-C.C. conducted the VLA and Keck observations, reduced and analysed the HST, Gemini and VLA data and performed GALFIT analysis and optical and NIR spectroscopic modelling. X.L. led the study, was PI of the Chandra, Gemini, HST and VLA observation programmes, conducted the Keck observations and reduced the Keck data. A.F. analysed Chandra data and performed BAYMAX analysis. Y.S. was PI of the Keck observation programme, conducted Keck observations and wrote the optical and NIR spectroscopic modelling pipeline. M.O. performed strong lensing mass model tests. N.C. performed cosmological simulations. X.L., Y.-C.C., A.F. and Y.S. co-wrote the manuscript with the help of N.C. and M.H. All authors contributed to the results and commented on the manuscript.

**Additional information**
**Supplementary information** The online version contains supplementary material available at https://doi.org/10.1038/s41586-023-05766-6.
**Correspondence and requests for materials** should be addressed to Xin Liu.
**Peer review information** *Nature* thanks A. Barnacka and the other, anonymous, reviewer(s) for their contribution to the peer review of this work.